In Vivo Evaluation of a PAMAM-Cystamine-(Gd-DO3A) Conjugate as a Biodegradable Macromolecular MRI Contrast Agent

RONGZUO XU,* YANLI WANG,* XULI WANG,* EUN-KEE JEONG,† DENNIS L. PARKER,† AND ZHENG-RONG LU*,[1]

Department of Pharmaceutics and Pharmaceutical Chemistry; and †Department of Radiology, University of Utah, Salt Lake City, Utah 84108

Macromolecular Gd(III) chelates are superior magnetic resonance imaging (MRI) contrast agents for blood pool and tumor imaging. However, their clinical development is limited by the safety concerns related to the slow excretion and long-term gadolinium tissue accumulation. A generation 6 PAMAM Gd(III) chelate conjugate with a cleavable disulfide spacer, PAMAM-G6-cystamine-(Gd-DO3A), was prepared as a biodegradable macromolecular MRI contrast agent with rapid excretion from the body. T_1 and T_2 relaxivities of the contrast agent were 11.6 and 13.3 $mM^{-1}sec^{-1}$ at 3T, respectively. Blood pool and tumor contrast enhancement of the agent were evaluated in female nude mice bearing MDA-MB-231 human breast carcinoma xenografts with a nondegradable conjugate PAMAM-G6-(Gd-DO3A) as a control. PAMAM-G6-cystamine-(Gd-DO3A) resulted in significant contrast enhancement in the blood for about 5 mins, and Gd-DO3A was released from the conjugate and rapidly excreted *via* renal filtration after the disulfide spacer was cleaved. The nondegradable control had much longer blood circulation and excreted more slowly from the body. PAMAM-G6-cystamine-(Gd-DO3A) also resulted in more prominent tumor contrast enhancement than the control. However, PAMAM-G6-cystamine-(Gd-DO3A) demonstrated high toxicity due to the intrinsic toxicity of PAMAM dendrimers. In conclusion, although PAMAM-G6-cystamine-(Gd-DO3A) showed some advantages compared with the nondegradable control, PAMAM dendrimers are not suitable carriers for biodegradable macromolecular MRI contrast agents, due to their high toxicity. Exp Biol Med 232:1081–1089, 2007

Key words: PAMAM; MRI contrast agents; disulfide spacer; biodegradable

Introduction

Magnetic resonance imaging (MRI) is a powerful imaging modality for visualizing soft tissues with high spatial resolution. Currently, about 25% of the MRI examinations use contrast agents to enhance image contrast between diseased tissues and normal tissues (1). MRI contrast agents approved for clinical applications are mostly low–molecular weight gadolinium(III) chelates, including Gd-DTPA, Gd-DOTA, and their derivatives. However, these agents rapidly extravasate from blood circulation and eliminate *via* renal filtration. As a result, they provide a transient time window for contrast-enhanced MRI examinations and have a limited efficacy in improving MR image quality. Macromolecular gadolinium(III) complexes have prolonged blood circulation and can preferentially accumulate in solid tumors due to the hyperpermeability of tumor vasculature (2). They have demonstrated superior contrast enhancement for MR angiography and cancer imaging in preclinical studies. Various macromolecular MRI contrast agents have been prepared by conjugating the gadolinium chelates to the polymer backbones, including polylysine (3), polysaccharides (4), dendrimers (5), and proteins (6). Unfortunately, clinical applications of these macromolecular contrast agents have been limited by their slow excretion and the potential toxicity due to long-term tissue accumulation of free gadolinium ions (7).

To alleviate the safety concerns regarding macromolecular MRI contrast agents, we have recently developed biodegradable macromolecular MR contrast agents to facilitate the excretion of contrast agents after MRI examinations. The biodegradable macromolecular MRI contrast agents are based on either polymer Gd(III) chelate conjugates with disulfide spacers or polydisulfide Gd(III) complexes in which disulfide bonds are incorporated into the polymer backbones (8–12). These novel, biodegradable, macromolecular MRI contrast agents behave initially as macromolecular agents and have longer blood circulation than low–molecular weight Gd(III) chelates. The disulfide

This work was supported in part by the National Institutes of Health grant CA097465.

[1] To whom correspondence should be addressed at 421 Wakara Way, Suite 318, Salt Lake City, UT 84108. E-mail: zhengrong.lu@utah.edu

Received February 15, 2007.
Accepted March 16, 2007.

DOI: 10.3181/0702-RM-33
1535-3702/07/2328-1081$15.00

bonds are gradually cleaved by endogenous free thiols in the plasma *via* thiol-disulfide exchange reactions. Consequently, the polydisulfide Gd(III) complexes are broken down into low–molecular weight chelates or are released as Gd(III) chelates from the polymer conjugates. These low–molecular weight chelates can be rapidly excreted from the body with minimal long-term tissue accumulation. Preclinical studies showed that these biodegradable macromolecular MRI contrast agents result in superior contrast enhancement for cardiovascular and tumor MR imaging. In addition, polydisulfide Gd(III) chelates were rapidly excreted, with minimal long-term tissue accumulation comparable to that of clinically used MRI contrast agents (13, 14). Poly(L-glutamic acid) Gd-DO3A conjugate with a disulfide spacer resulted in significant reduction of Gd(III) tissue accumulation compared with poly(L-glutamic acid) Gd-DO3A conjugate with a nondegradable spacer (15). However, the long-term Gd(III) tissue accumulation with poly(L-glutamic acid) Gd-DO3A conjugate with the disulfide spacer was still considerably high compared with clinical contrast agents, possibly due to steric hindrance of the coiled structure of linear polymers that might inhibit complete cleavage reaction of the disulfide spacer in the conjugate. Therefore, it is of great interest to investigate macromolecular Gd(III) chelate conjugates with the disulfide spacer located on surface of the macromolecular structures, where steric hindrance is minimal and the disulfide bonds are readily cleaved to release Gd(III) chelates from the conjugate.

Dendrimers are hyperbranched spherical macromolecules with well-defined unimolecular architectures and a high density of functional groups on the surface. Macromolecular MRI contrast agents prepared from dendrimers have several advantages over linear polymers, including uniform molecular weight distribution, relatively controlled structure, high relaxivities, and high loading of Gd(III) chelates on the surface (16). Depending on their sizes and cores, macromolecular MRI contrast agents based on PAMAM dendrimers have shown pharmacokinetic properties (5, 17, 18). Preclinical studies have shown that PAMAM-based macromolecular contrast agents are effective for contrast-enhanced MR tumor imaging, liver imaging, renal imaging, angiography, and lymphography (19, 20). Clinical development of PAMAM-based contrast agents is also limited by the safety concerns related to their slow excretion (21). The conjugation of Gd(III) chelates to PAMAM dendrimers *via* a degradable disulfide spacer may facilitate the excretion of contrast agents after the MRI examinations. Since dendrimers have a spherical structure and Gd(III) chelates are conjugated to the surface of the dendrimers, the cleavage reaction of the disulfide spacer in the conjugate will be fast, due to low steric hindrance. Dendrimer Gd(III) chelate conjugates with the degradable spacer will show more complete excretion than the corresponding linear polymer conjugates.

In this study, we synthesized a generation 6 PAMAM Gd-DO3A conjugate with a cystamine spacer, PAMAM-G6-cystamine-(Gd-DO3A), and evaluated its potential as a biodegradable macromolecular MRI contrast agent in an animal tumor model. A generation 6 PAMAM Gd-DO3A conjugate with a nondegradable spacer was synthesized and used as a control. The new biodegradable macromolecular contrast agent had relatively high relaxivities at 3T. PAMAM-G6-cystamine-(Gd-DO3A) resulted in significant contrast enhancement in tumor tissue and cleared more rapidly from the blood circulation than the control agent.

Materials and Methods

Bromoacetic acid, mono-Boc-ethylenediamine, *N*-hydroxysuccinimide, triethylene amine (TEA), and *N*-diisopropylethylamine (DIEA) were purchased from Lancaster Synthesis Inc. (Pelham, NH). Gadolinium acetate and *tert*-butyl bromoacetate were purchased from Alfa Aesar (Ward Hill, MA). EDTA dipotassium salt and 1,1′-thiocarbonyldi-2,2′-pyridone were purchased from Sigma-Aldrich (St. Louis, MO). MDA-MB-231 human breast carcinoma cell line, Leibovitz's L-15 medium with 2 m*M* L-glutamine, and fetal bovine serum were purchased from the American Type Culture Collection (Manassas, VA). Matrigel was purchased from BD Sciences (San Jose, CA). The Spectra/Por 6 membrane (MWCO 2000) was purchased from Spectrum Laboratory (Rancho Dominguez, CA). 1,4,7,10-Tetraazacyclododecane-1,4,7-tris(acetic acid t-butyl ester) (TB-cyclen) and 1,4,7,10-tetraazacyclododecane-1,4,7-tris(acetic acid)-10-(acetic acid-cystamine monoamide) (DO3A-cystamine) were prepared according to the literature (15).

Synthesis. *N-Boc-N′-Bromoacetylethylenediamine.* *N*-Boc-ethylenediamine (1.6 g, 13 mmol) in dichloromethane (80 ml) was added dropwise to a solution of bromoacetic acid *N*-hydroxysuccinimide ester (3.1 g, 13 mmol) in dichloromethane (60 ml) while stirring at 0°C. The reaction mixture was stirred for 24 hrs at 25°C. The reaction mixture was washed with 0.1 *N* NaOH aqueous solution (2×50 ml) and water (2×50 ml). The organic layer was dried with anhydrous Na_2SO_4 and concentrated. The final product was purified by silica gel chromatography eluted with 25% to 50% ethyl acetate in hexane. The product (2.08 g) was obtained with a yield of 74%. ESI-MS (m/z, $[M+H]^+$): 282.04 (observed), 282.04 (calculated). ^1H NMR, δ_H ($CDCl_3$, ppm): 7.16 (s, 1H, NHCOO), 4.97 (s, 1H, CONH), 3.84 (s, 2H, $BrCH_2CO$), 3.37 (m, 2H, CH_2NHCOO), 3.30 (t, 2H, $CONHCH_2$), 1.42 (s, 9H, $COO(CH_3)_3$).

1,4,7,10-Tetraazacyclododecane-1,4,7-Tris-(Acetic Acid)-10-(Acetic Acid-1,2-Ethylenediamine Monoamide) (DO3A-EA). TB-cyclen (0.94 g, 1.8 mmol) and excess K_2CO_3 (0.76 g, 5.6 mmol) were mixed in acetonitrile (60 ml). Then, *N*-Boc-*N′*-bromoacetylethylenediamine (0.51 g, 1.8 mmol) in acetonitrile (30 ml) was added dropwise within 30 mins. The reaction mixture was stirred for 24 hrs at room temperature. The inorganic precipitate was filtered off, and the solvent was evaporated under vacuum. The residue was

then dried under vacuum. The Boc protection was removed by dissolving the residue in a minimum amount of cold trifluoroacetic acid for 24 hrs. Trifluoroacetic acid was then evaporated under vacuum, and the residue was treated with ether. The precipitate was collected, washed with ether, and dried under vacuum. Yield: 1.08 g, 89%. ESI-MS (m/z, $[M+H]^+$): 447.3 (measured), 447.3 (calculated).

1,4,7,10-Tetraazacyclododecane-1,4,7-Tris-(Acetic Acid)-10-(Acetic Acid-2-Isothiocyanatoethyl Amide) (DO3A-EA-NCS). DO3A-EA (100 mg, 0.22 mmol) in a mixture of 2.0 ml DMSO and 1.0 ml TEA was added dropwise into 1,1′-thiocarbonyldi-2,2′-pyridone (260 mg, 1.1 mmol) in 2.0 ml DMSO in 30 mins. The reaction was stirred for another 30 mins at room temperature. The product was precipitated from a mixture of acetone/diethyl ether (1:3 v/v), collected by filtration and washed with the solvent mixture. Yield: 90 mg, 80%. ESI-MS (m/z, $[M+H]^+$): 489.20 (measured), 489.21 (calculated).

1,4,7,10-Tetraazacyclododecane-1,4,7-Tris-(Acetic Acid)-10-(Acetic Acid-Isothiocyanatocystamine Monoamide) (DO3A-SS-NCS). DO3A-SS-NCS was similarly prepared from DO3A-cystamine (100 mg, 0.19 mmol) and 1,1′-thiocarbonyldi-2,2′-pyridone (260 mg, 1.1 mmol) according the method described above. Yield: 91 mg, 85%. ESI-MS (m/z): 581.10 ($[M+H]^+$, measured), 581.18 (calculated).

PAMAM-G6-(Gd-DO3A) and PAMAM-G6-Cystamine-(Gd-DO3A). Generation 6 PAMAM dendrimer was dissolved in water at a concentration of 10 mg/ml, and a 256-molar excess of DO3A-EA-NCS or DO3A-SS-NCS was added to the solution. Final pH of the mixture was adjusted to 9 with 1.0 *M* NaOH. The reaction was stirred at room temperature for 24 hrs. Then, another 256-molar excess of DO3A-EA-NCS or DO3A-SS-NCS was added, with pH maintained at 9, and the reaction was stirred for another 24 hrs. The step was repeated once more to ensure complete reaction. The PAMAM-DO3A conjugates were purified by dialysis with a membrane of molecular weight cutoff of 2000 Daltons against de-ionized water for 48 hrs and were obtained after lyophilization. The ligand conjugates were then reacted with a large excess (512 molar excess) of $Gd(OAc)_3$ in 0.3 *M* (pH 5) citric acid buffer. The reaction mixture was stirred at room temperature for 72 hrs. EDTA was added, and the mixture was stirred for additional 1 hr. The mixtures were dialyzed against de-ionized water for 48 hrs. The final products were obtained after lyophilization. The gadolinium contents in the conjugates ware measured by inductively coupled plasma optical emission spectroscopy (ICP-OES; Perkin-Elmer Optima 3100XL; Norwalk, CT) at 342 nm.

Relaxivities. The r_1 and r_2 relaxivities of the gadolinium in the contrast agents were measured on a Siemens Trio 3T MRI scanner (München, Germany). The T_1 relaxation time was measured using a standard inversion recovery (IR)–prepared turbo spin echo (TSE) sequence. Three different concentrations of each sample were prepared in triplicate, placed at triplets, placed inside a birdcage human head coil, and scanned with a series of inversion times (TIs) from 22 ms to 1600 ms. The net magnetization (M_{TI}) for at each TI was calculated from the region of interest (ROI) using Osirix (http://homepage.mac.com/rossetantoine/osirix/) software. T_1 relaxation time was calculated by nonlinear regression fitting of equation 1: $M_{TI} = M_o \times (1 - 2\exp(-TI/T_1))$, where M_{TI} is the net magnetization at time TI; TI is the inversion time; and M_o is the initial magnetization. Relaxivity r_1 was determined as the slope of the plot of $1/T_1$ *versus* $[Gd^{3+}]$. The samples were also scanned using a TSE imaging sequence with turbo factor 3 to measure T_2 relaxation time. The parameters were: TE = 12, 24, 36, 47, 59, 71, 83, 95, and 107 ms; and TR = 3000 ms. T_2 values were calculated from equation 2: $M_z = M_0 \times \exp(-TE/T_2)$, where M_z is the net magnetization for each TE. Relaxivity r_2 was determined as the slope of $1/T_2$ *versus* $[Gd^{3+}]$ plot.

Animal Tumor Model. Female athymic nude mice (5 weeks old, ~22–25 g; Charles River Laboratories, Wilmington, MA) were cared for under a protocol approved by the University of Utah Institutional Animal Care and Use Committee. MDA-MB-231 human breast carcinoma cells were cultured in Leibovitz's L-15 medium with 2 m*M* L-glutamine and 5% fetal bovine serum at 37°C in a humidified atmosphere with 5% CO_2. The aliquots of 0.2 ml Matrigel mixture containing 1.6 million cells were implanted subcutaneously in both flanks of the mice. Each implant generated a tumor 0.7–1.0 cm in diameter after growing for 4 weeks.

MR Imaging. The mice were anesthetized by intraperitoneal administration of a mixture of xylazine (12 mg/kg) and ketamine (80 mg/kg). The contrast agents were injected intravenously through a tail vein at the dose of 0.1 mmol Gd/kg. Three mice were used for each contrast agent. The mice were placed in a wrist coil, and the MR images were acquired before and 2, 5, 10, 15, 30, and 60 mins after the injection of the contrast agents on a Siemens Trio 3T scanner. A 3D-FLASH pulse sequence was used to acquire whole-body images, and a 2D T_1-weighted spin echo sequence was used to acquire axial tumor images. The 3D-FLASH sequence parameters were 2.74-ms echo time (TE), 7.75-ms repetition time (TR), 25° flip angle, 120-mm field of view (FOV), and 0.5-mm coronal slice thickness. The spin-echo sequence parameters were 8.90-ms TE, 400-ms TR, 90° flip angle, and the 2-mm axial slice thickness. MR images were analyzed with Osirix (http://homepage.mac.com/rossetantoine/osirix/) software. The regions of interest (ROIs) in each mouse were set at the left ventricle, representing blood in the heart and the liver in 3D-FLASH images, and the tumor rim and tumor interstitium in the spin-echo images. The relative signal intensities were calculated as the ratios of signal intensities of postinjection to that of preinjection in corresponding ROIs.

Biodistribution Study. The mice were sacrificed by CO_2 at 10 days after injection of the agents, and the Gd(III)

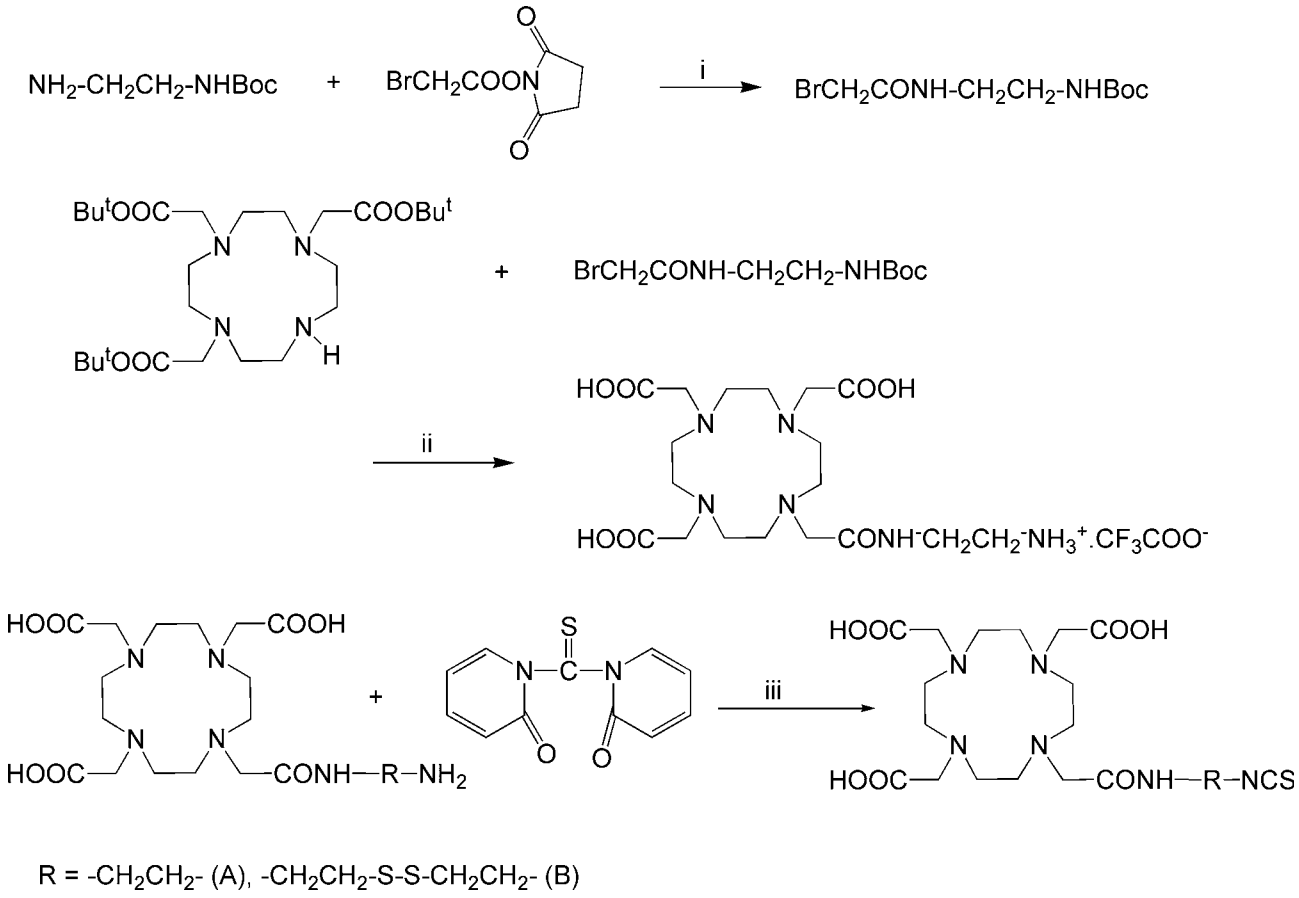

Scheme 1. Synthesis of ligands DO3A-EA-NCS (A) and DO3A-SS-NCS (B). (i) CH_2Cl_2, rt, overnight; (ii) trifluoroacetic acid, rt, 24 hrs; (iii) DMSO, TEA, rt, 1 hr.

accumulation in these mice was investigated. The mice injected with PAMAM-G6-cystamine-(Gd-DO3A) died within 24 hrs after MRI studies due to toxicity of the PAMAM dendrimer; the Gd(III) tissue accumulation in these mice was not investigated. Tissue and organ samples, including femur, heart, lung, liver, muscle, spleen, and kidneys, were collected and weighed. All the samples were treated by ultrapure nitric acid (70%; EMD, Gibbstown, NJ) with 1.0 ml for the liver and 0.5 ml for all other tissue samples. The tissue samples liquefied after 4 to 5 days. The mixtures were diluted three to four times with distilled water and then centrifuged at 20,000 *g* for 15 mins. The supernatant was collected and filtered through a 0.2-μm filter. The gadolinium content in the filtrate was determined by ICP-OES. Since whole organs or tissues were collected, the gadolinium contents deposited in the lung, heart, liver, spleen, both kidneys, and tumor were directly determined by ICP-OES measurements. The gadolinium residuals in the femur and muscle were calculated based on the estimation that the femur and muscle accounted for 0.4% and 40% of the body weight, respectively (22). The gadolinium retention in the tissue and organs was expressed as the percentage of the injected doses.

Data Analysis and Statistics. Statistical analysis was performed using Student's *t*-test with Prism 4 software (GraphPad Software, San Diego, CA). For all statistical analyses, the difference was considered significant when $P < 0.05$.

Results

The synthesis of the PAMAM Gd-(DO3A) conjugate with degradable spacer PAMAM-G6-cystamine-(Gd-DO3A) and the nondegradable control PAMAM-G6-(Gd-DO3A) is described in Schemes 1 and 2. Gd-DO3A was used as the contrast agent because of its high thermodynamic and kinetic stability. DO3A derivatives with different spacers and a reactive isothiocyanato group, DO3A-EA-NCS and DO3A-SS-NCS, were first prepared (23) and then conjugated to the G6 PAMAM dendrimer by reacting the isothiocyanato group with the amino groups of the dendrimer. An excess of DO3A derivatives was used to achieve high conjugation degree. The physicochemical properties of the conjugates are listed in Table 1. A relatively high conjugation degree (approximately 75%) was achieved for both conjugates. Both PAMAM-G6-cystamine-(Gd-DO3A) and PAMAM-G6-(Gd-DO3A) have higher T_1 and T_2 relaxivities per Gd chelate than Gd-

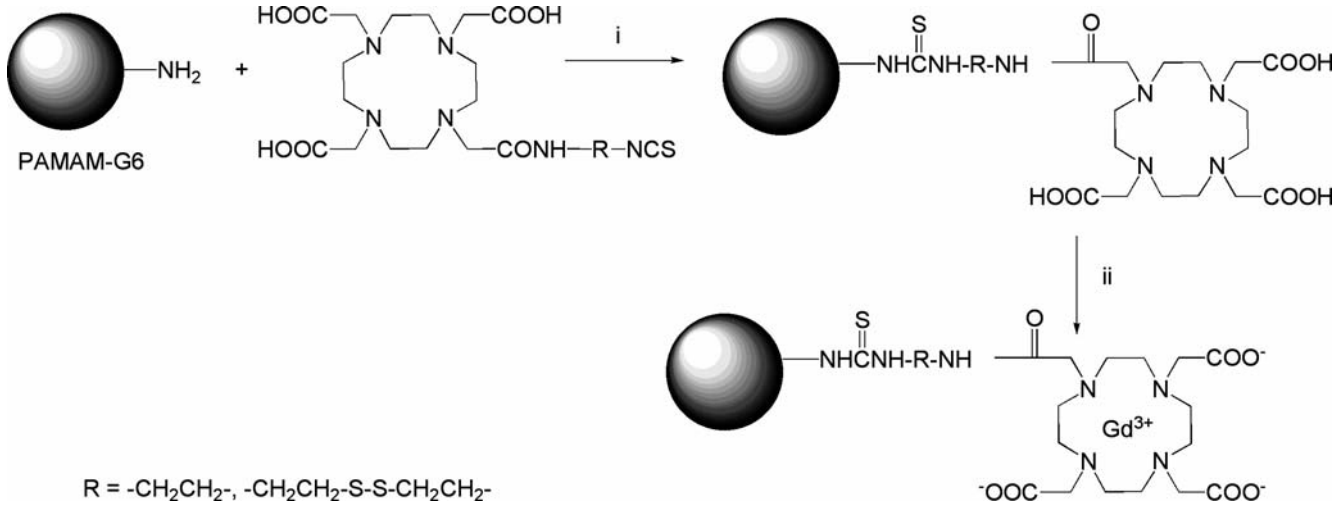

Scheme 2. Synthesis of PAMAM-G6-(Gd-DO3A) and PAMAM-G6-cystamine-(Gd-DO3A). (i) Water, pH 9, 72 hrs; (ii) gadolinium acetate, pH 5, 72 hrs; EDTA, 1 hr.

DO3A (24) and poly(L-glutamic acid)-cystamine-(Gd-DO3A) (15).

Contrast-enhanced MRI with PAMAM-G6-cystamine-(Gd-DO3A) was investigated in female nude mice bearing MDA-MB-231 human breast carcinoma xenografts using PAMAM-G6-(Gd-DO3A) as a control. Figure 1 shows the 3-D maximum intensity projection (MIP) MR images of mice before and at various time points after the administration of the contrast agents at a dose of 0.1 mmol Gd/kg. All mice in the group injected with the same contrast agent showed similar contrast enhancement. Significant contrast enhancement was observed in the blood and the heart during the first 5 mins after injection of PAMAM-G6-cystamine-(Gd-DO3A) and then rapidly decreased. Significant enhancement in the heart was still visible at 60 mins after the injection of the nondegradable agent PAMAM-G6-(Gd-DO3A). PAMAM-G6-cystamine-(Gd-DO3A) also resulted in less enhancement in the liver than the control conjugate. Analysis of relative signal intensities in the blood and liver showed that PAMAM-G6-cystamine-(Gd-DO3A) had more rapid blood clearance and lower liver uptake than PAMAM-G6-(Gd-DO3A) ($P < 0.05$; Fig. 2). Both agents resulted in strong enhancement in the kidneys. Strong enhancement was observed in the bladder of the mice injected with PAMAM-G6-cystamine-(Gd-DO3A) starting at 10 mins after injection, whereas only slight enhancement was observed for the control. The results indicate that the disulfide spacer in PAMAM-G6-cystamine-(Gd-DO3A) was rapidly cleaved *in vivo* to release the Gd(III) chelates from the conjugate. The released low molecular chelate rapidly excreted *via* renal filtration and accumulated in the urinary bladder. In comparison, the control conjugate with nondegradable spacer had long blood circulation and slow excretion.

Both conjugates resulted in significant tumor enhancement in the 3-D MIP images (Fig. 1) and the axial 2-D spin-echo images of the mice bearing MDA-MB-231 human breast carcinoma xenografts (Fig. 3). Detailed analysis of relative signal intensities in tumors of the spin-echo images showed that PAMAM-G6-cystamine-(Gd-DO3A) resulted in stronger enhancement than the control (Fig. 4). High signal was observed in the tumor periphery for both agents compared with that in the tumor interstitium, possibly due to tumor necrosis in the inner tumor tissue. PAMAM-G6-cystamine-(Gd-DO3A) seems to be more effective in contrast-enhanced tumor imaging than the nondegradable control.

Unfortunately, the mice injected with PAMAM-G6-cystamine-(Gd-DO3A) died within 24 hrs after injection. Postmortem examinations revealed severe hemolysis in the

Table 1. Physicochemical Parameters of PAMAM-G6-(Gd-DO3A) and PAMAM-G6-Cystamine-(Gd-DO3A)

	r_1 per Gd^{3+} ($mM^{-1}sec^{-1}$)[a]	r_2 per Gd^{3+} ($mM^{-1}sec^{-1}$)[a]	Gd content (w/w)[b]	Gd^{3+} no. per dendrimer[c]	Total r_1 ($mM^{-1}sec^{-1}$)[d]	Total r_2 ($mM^{-1}sec^{-1}$)[d]
PAMAM-G6-(Gd-DO3A)	11.6	13.3	12.40%	193	2238.8	2566.9
PAMAM-G6-SS-(Gd-DO3A)	11.1	12.2	11.35%	195	2164.5	2379

[a] Determined on a Siemens Trio 3T scanner.
[b] Determined by ICP-OES.
[c] Estimated from comparing the gadolinium content with the theoretical value.
[d] Calculated relaxivity per dendrimer.

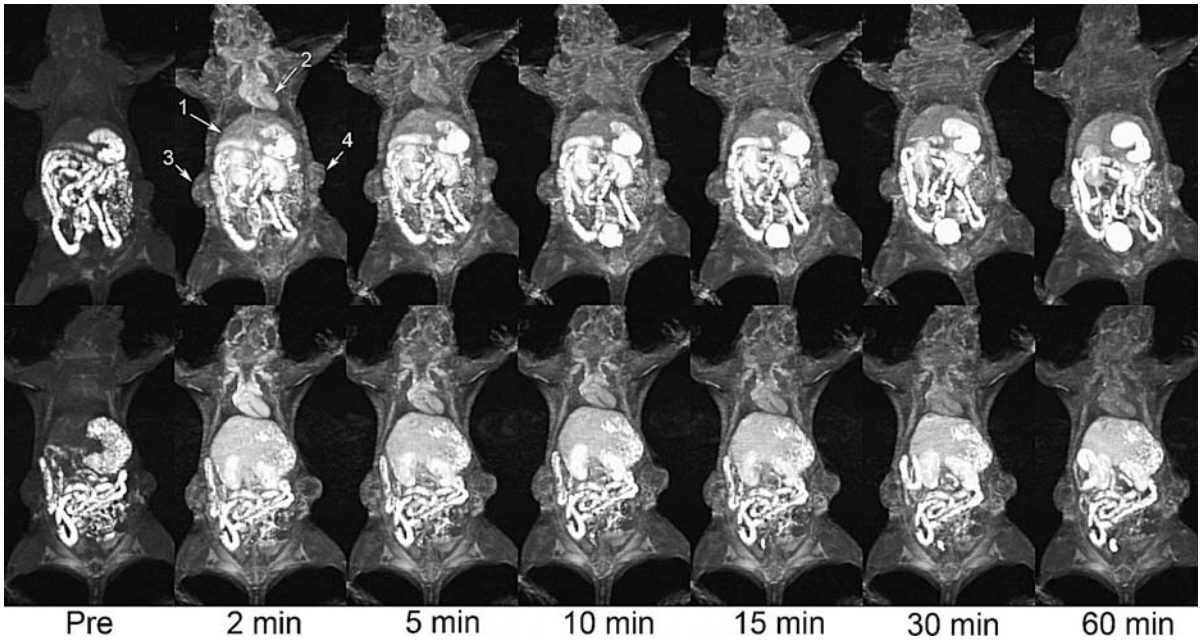

Figure 1. Contrast-enhanced 3-D maximum intensity projection (3D-MIP) MR images of tumor-bearing mice before and at various time points after intravenous injection of PAMAM-G6-cystamine-(Gd-DO3A) (top row) and PAMAM-G6-(Gd-DO3A) (bottom row) at the dose of 0.1 mmol Gd/kg. Arrows point to the (1) liver, (2) heart, and (3) and (4) tumors.

liver and intestine. The three mice injected with non-degradable PAMAM-G6-Gd-DO3A survived, and they were sacrificed 10 days after injection for determination of long-term Gd(III) tissue accumulation. Figure 5 depicts the residual gadolinium content in major organs and tissues, including the femur, heart, kidneys, liver, lung, muscle, spleen, and tumor, expressed as percentage of the original injected dose. High Gd(III) retentions were observed in the liver, muscle, spleen, and kidney for PAMAM-G6-Gd-DO3A, which were much higher than those of low–molecular weight Gd-(DTPA-BMA) and the polydisulfide-based biodegradable macromolecular contrast agents (13, 14).

Discussion

PAMAM-G6-cystamine-(Gd-DO3A) was prepared and evaluated as a new biodegradable macromolecular MRI contrast agent. Because the reactive amino groups were exposed at the surface of the dendrimer, a relatively high conjugate degree (approximately 75%) was achieved in the preparation of PAMAM-G6-cystamine-(Gd-DO3A), much higher than that of poly(L-glutamic acid)-cystamine-(Gd-DO3A) conjugate (approximately 55%; Ref. 15). The dendrimer conjugate also had higher relaxivities than the linear polymer conjugate at 3T. Since macromolecules can preferentially accumulate in solid tumor tissue due to the hyperpermeability of tumor vasculature, high loading of Gd(III) chelate in the macromolecules could increase tumor concentration of contrast agents. High relaxivity and high local concentration of contrast agents could result in strong contrast enhancement in tumor tissues.

The MRI study showed that PAMAM-G6-cystamine-

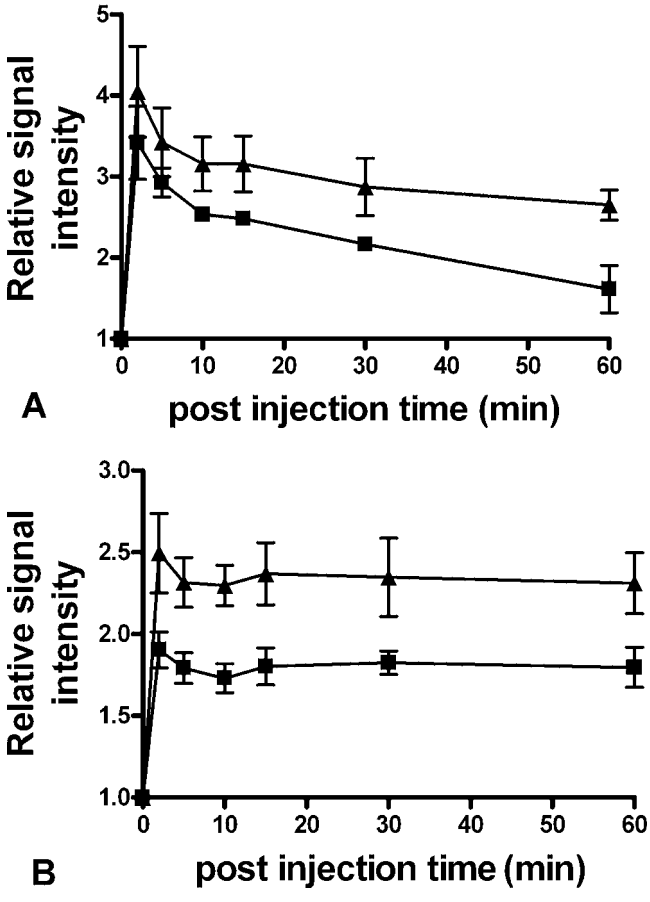

Figure 2. Relative signal intensities in the blood (A) and liver (B) before and at various time points after the injection of PAMAM-G6-(Gd-DO3A) (black triangles) and PAMAM-G6-cystamine-(Gd-DO3A) (black squares).

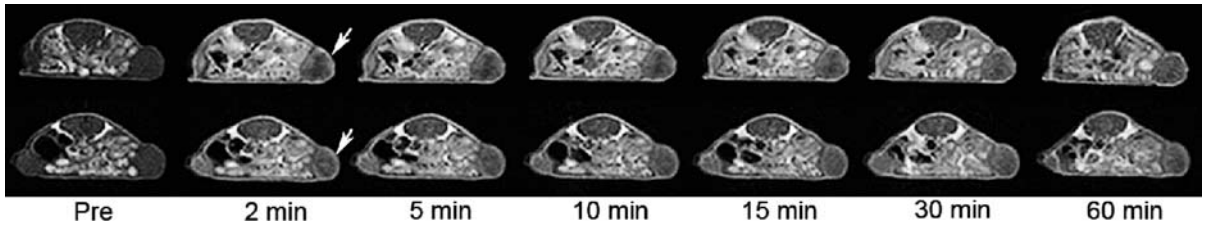

Figure 3. T_1-weighted spin echo images of axial tumor-bearing mice body before injection and at various time points after injection of PAMAM-G6-cystamine-(Gd-DO3A) (top row) and PAMAM-G6-(Gd-DO3A) (bottom row). Arrows point to the tumor.

(Gd-DO3A) was effective for prolonged blood pool and tumor contrast enhancement (approximately 5 mins) in mice and then cleared more rapidly from the blood circulation than the nondegradable control. The cleavage of the disulfide spacer released Gd(III) chelates from the conjugate and facilitated the rapid blood clearance. Rapid release of Gd(III) chelates from PAMAM-G6-cystamine-(Gd-DO3A) also resulted in much lower liver contrast enhancement than the nondegradable control. Dynamic MR images revealed that the released Gd(III) chelates excreted *via* renal filtration and accumulated in the urinary bladder. It appears that the blood clearance of Gd(III) chelate in PAMAM-G6-cystamine-(Gd-DO3A) was much faster than linear polymer conjugate poly(L-glutamic acid)-cystamine-(Gd-DO3A). For the latter agent, strong enhancement was still visible in the blood of mice 2 hrs after the injection at a much lower dose (0.04 mmol Gd/kg), whereas the former agent only resulted in significant enhancement in less than 10 mins at a higher dose (0.1 mmol Gd/kg). The results validated our hypothesis that Gd(III) chelates conjugated to dendrimer with disulfide spacers could be more rapidly released than those in linear polymer conjugates because of low steric hindrance in the dendrimer conjugates. The biodegradable PAMAM-G6-cystamine-(Gd-DO3A) had stronger contrast enhancement than the nondegradable control in the tumor periphery, suggesting that the released Gd-DO3A derivative also entered the tumor. The diffusion of the released agent into tumor tissue would be at a much faster rate than that of the macromolecular agent, as expected from direct comparison of Gd-DTPA and the albumin-$(Gd\text{-}DTPA)_{30}$ in a breast tumor model (25).

Unfortunately, PAMAM-G6-cystamine-(Gd-DO3A) exhibited high toxicity, and the mice injected with the conjugate died 3 to 24 hrs after the tail vein injection. The high toxicity might be caused by the hemotoxicity of the G6 PAMAM dendrimer after the complete release of Gd(III) chelates. It is known that PAMAM dendrimers can cause hemolysis and erythrocyte deformation and aggregation (26, 27). The MRI study showed that most of the Gd(III) chelates in PAMAM-G6-cystamine-(Gd-DO3A) were rap-

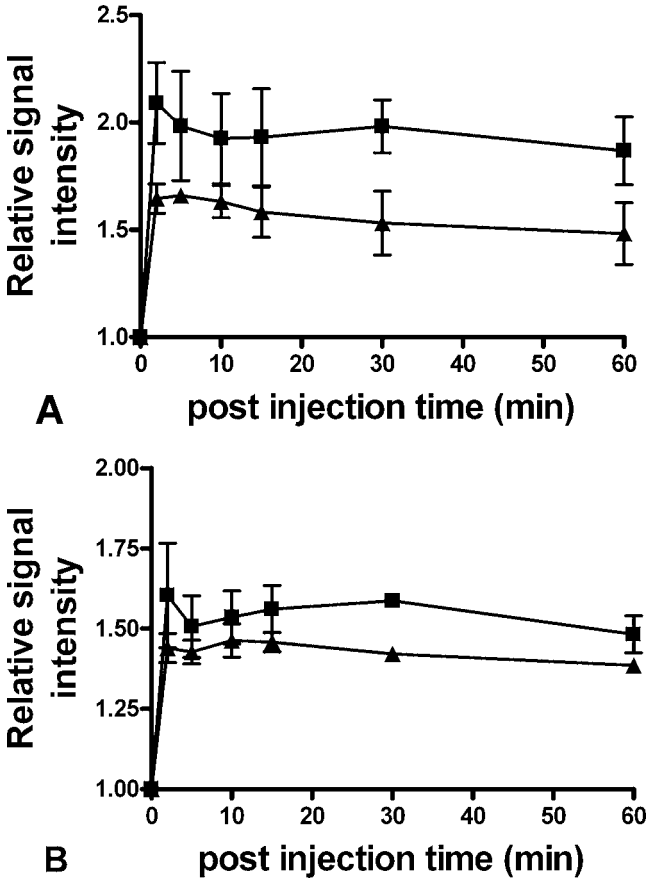

Figure 4. Relative signal intensities in (A) tumor periphery and (B) tumor interstitium before and at various time points after the injection of PAMAM-G6-cystamine-(Gd-DO3A) (black squares) and PAMAM-G6-(Gd-DO3A) (black triangles) at the dose 0.1 mmol Gd/kg.

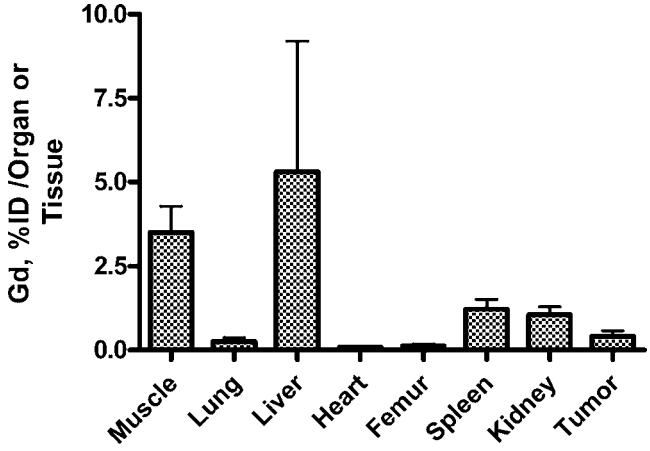

Figure 5. Gadolinium residuals in the main organ and tissues in nude mice bearing MDA-MB-231 xenografts 10 days after injection of PAMAM-G6-(Gd-DO3A).

idly released and eliminated within 1 hr after injection, which left naked PAMAM dendrimer derivatives circulating in the blood. Postmortem examinations revealed severe hemolysis in the liver and intestine, which confirmed the hemotoxicity of high-generation PAMAM dendrimers. No obvious toxicity was observed for poly(L-glutamic acid)-cystamine-(Gd-DO3A) in mice (15). The nondegradable control also did not show obvious signs of toxicity, consistent with the nondegradable PAMAM-based MRI contrast agents reported by other groups (19–21). Gd(III) chelates on the surface of the nondegradable control might shield the interaction of the cationic core with blood cells. However, the nondegradable PAMAM conjugate excreted slowly from the body and resulted in high long-term gadolinium tissue accumulation.

This study showed that the dendrimer conjugate with a disulfide spacer clearly had some advantageous features compared with linear polymer conjugates, including high relaxivity, high contrast agent loading, rapid excretion of the contrast agents from the body, effective contrast-enhanced blood pool, and tumor imaging. However, high-generation PAMAM dendrimers have high intrinsic toxicity and are not suitable as carriers for biodegradable macromolecular MRI contrast agents. Although there have been some efforts to reduce the toxicity of PAMAM dendrimers by chemical modification of the dendrimer surface with polyethylene glycol (28, 29), it would be better to choose nontoxic dendrimers to design and develop biodegradable dendrimeric MRI contrast agents. Currently, we focus on using nontoxic dendrimers to design and develop biodegradable macromolecular MRI contrast agents.

Conclusions. The generation 6 PAMAM-cystamine-(Gd-DO3A) conjugate resulted in rapid excretion of Gd(III) chelates from the body *via* renal filtration after the cleavage of the disulfide spacer. The conjugate was effective for contrast-enhanced blood pool imaging and tumor imaging. However, the conjugate is not suitable for further development as a biodegradable macromolecular MRI contrast agent because of its high toxicity related to the intrinsic hemotoxicity of PAMAM dendrimers.

We are grateful for the technical support from Dr. Yongen Sun and Ms. Melody Johnson.

1. The Medical and Healthcare Marketplace Guide (20th ed.). Philadelphia, PA: Dorland Healthcare Information, 2005.
2. Maeda H, Seymour LW, Miyamoto Y. Conjugates of anticancer agents and polymers: advantages of macromolecular therapeutics in vivo. Bioconjug Chem 3:351–362, 1992.
3. Schuhmann-Giampieri G, Schmitt-Willich H, Frenzel T, Press WR, Weinmann HJ. In vivo and in vitro evaluation of Gd-DTPA-polylysine as a macromolecular contrast agent for magnetic resonance imaging. Invest Radiol 26:969–974, 1991.
4. Rongved P, Klaveness J. Water-soluble polysaccharides as carriers of paramagnetic contrast agents for magnetic resonance imaging: synthesis and relaxation properties. Carbohydr Res 214:315–323, 1991.
5. Bryant LH Jr., Brechbiel MW, Wu C, Bulte JW, Herynek V, Frank JA. Synthesis and relaxometry of high-generation (G = 5, 7, 9, and 10) PAMAM dendrimer-DOTA-gadolinium chelates. J Magn Reson Imaging 9:348–352, 1999.
6. Lauffer RB, Brady TJ. Preparation and water relaxation properties of proteins labeled with paramagnetic metal chelates. Magn Reson Imaging 3:11–16, 1985.
7. Franano FN, Edwards WB, Welch MJ, Brechbiel MW, Gansow OA, Duncan JR. Biodistribution and metabolism of targeted and nontargeted protein-chelate-gadolinium complexes: evidence for gadolinium dissociation in vitro and in vivo. Magn Reson Imaging 13:201–214, 1995.
8. Lu Z, Wang X, Parker D, Goodrich K, Buswell H. Poly(L-glutamic acid) Gd(III)-DOTA conjugate with a degradable spacer for magnetic resonance imaging. Bioconjug Chem 14:715–719, 2003.
9. Lu Z, Parker D, Goodrich K, Wang X, Dalle J, Buswell H. Extracellular biodegradable macromolecular gadolinium(III) complexes for MRI. Magn Reson Med 51:27–34, 2004.
10. Zong Y, Wang X, Goodrich K, Mohs A, Parker D, Lu Z. Contrast-enhanced MRI with new biodegradable macromolecular Gd(III) complexes in tumor-bearing mice. Magn Reson Med 53:835–842, 2005.
11. Kaneshiro T, Ke T, Jeong E, Parker D, Lu Z. Gd-DTPA L-cystine bisamide copolymers as novel biodegradable macromolecular contrast agents for MR blood pool imaging. Pharm Res 23:1285–1294, 2006.
12. Mohs A, Wang X, Goodrich K, Zong Y, Parker D, Lu Z. PEG-g-poly(GdDTPA-co-L-cystine): A biodegradable macromolecular blood pool contrast agent for MR imaging. Bioconjug Chem 15:1424–1430, 2004.
13. Wang X, Feng Y, Ke T, Schabel M, Lu Z. Pharmacokinetics and tissue retention of (Gd-DTPA)-cystamine copolymers, a biodegradable macromolecular magnetic resonance imaging contrast agent. Pharm Res 22:596–602, 2005.
14. Feng Y, Zong Y, Ke T, Lu ZR. Pharmacokinetics and blood pool contrast enhancement of Gd-DTPA cystine copolymers and Gd-DTPA cystine diethyl ester copolymers. Pharm Res 23:1736–1742, 2006.
15. Ke T, Feng Y, Guo J, Parker D, Lu Z. Biodegradable cystamine spacer facilitates the clearance of Gd(III) chelates in poly(glutamic acid) Gd-DO3A conjugates for contrast-enhanced MR imaging. Magn Reson Imaging 24:931–940, 2006.
16. Kobayashi H, Brechbiel MW. Dendrimer-based macromolecular MRI contrast agents: characteristics and application. Mol Imaging 2:1–10, 2003.
17. Kobayashi H, Sato N, Kawamoto S, Saga T, Hiraga A, Haque TL, Ishimori T, Konishi J, Togashi K, Brechbiel MW. Comparison of the macromolecular MR contrast agents with ethylenediamine-core versus ammonia-core generation-6 polyamidoamine dendrimer. Bioconjug Chem 12:100–107, 2001.
18. Rudovsky J, Botta M, Hermann P, Hardcastle KI, Lukes I, Aime S. PAMAM dendrimeric conjugates with a Gd-DOTA phosphinate derivative and their adducts with polyaminoacids: the interplay of global motion, internal rotation, and fast water exchange. Bioconjug Chem 17:975–987, 2006.
19. Sato N, Kobayashi H, Hiraga A, Saga T, Togashi K, Konishi J, Brechbiel MW. Pharmacokinetics and enhancement patterns of macromolecular MR contrast agents with various sizes of polyamidoamine dendrimer cores. Magn Reson Med 46:1169–1173, 2001.
20. Kobayashi H, Shirakawa K, Kawamoto S, Saga T, Sato N, Hiraga A, Watanabe I, Heike Y, Togashi K, Konishi J, Brechbiel MW, Wakasugi H. Rapid accumulation and internalization of radiolabeled herceptin in an inflammatory breast cancer xenograft with vasculogenic mimicry predicted by the contrast-enhanced dynamic MRI with the macromolecular contrast agent G6-(1B4M-Gd)(256). Cancer Res 62:860–866, 2002.
21. Kobayashi H, Kawamoto S, Jo SK, Bryant HL Jr, Brechbiel MW, Star RA. Macromolecular MRI contrast agents with small dendrimers:

pharmacokinetic differences between sizes and cores. Bioconjug Chem 14:388–94, 2003.

22. Parmelee DJ, Walovitch RC, Ouellet HS, Lauffer RB. Preclinical evaluation of the pharmacokinetics, biodistribution, and elimination of MS-325, a blood pool agent for magnetic resonance imaging. Invest Radiol 32:741–747, 1997.
23. Bloodworth AJ, Melvin T. 1, 1'-Thiocarbonyldi-2, 2'-pyridone: a new useful reagent for functional group conversions under essentially neutral conditions. J Org Chem 51:2613–2615, 1986.
24. Kang SI, Ranganathan RS, Emswiler JE, Kumar K, Gougoutas JZ, Malley MF, Tweedle MF. Synthesis, characterization, and crystal structure of the gadolinium(III) chelate of (1R,4R,7R)-.alpha.,.alpha.',.alpha.''-trimethyl-1,4,7,10-tetraazacyclododecane-1,4,7-triacetic acid (DO3MA). Inorg Chem 32:2912–2918, 1993.
25. Turetschek K, Huber S, Helbich T, Floyd E, Tarlo KS, Roberts TP, Shames DM, Wendland MF, Brasch RC. Dynamic MRI enhanced with albumin-(Gd-DTPA)30 or ultrasmall superparamagnetic iron oxide particles (NC100150 injection) for the measurement of microvessel permeability in experimental breast tumors. Acad Radiol 9:S112–S114, 2002.
26. Malik N, Wiwattanapatapee R, Klopsch R, Lorenz K, Frey H, Weener JW, Meijer EW, Paulus W, Duncan R. Dendrimers: relationship between structure and biocompatibility in vitro, and preliminary studies on the biodistribution of 125I-labelled polyamidoamine dendrimers in vivo. J Control Release 65:133–148, 2000.
27. Domanski DM, Klajnert B, Bryszewska M. Influence of PAMAM dendrimers on human red blood cells. Bioelectrochemistry 63:189–191, 2004.
28. Jevprasesphant R, Penny J, Jalal R, Attwood D, McKeown NB, D'Emanuele A. The influence of surface modification on the cytotoxicity of PAMAM dendrimers. Int J Pharm 252:263–266, 2003.
29. Kobayashi H, Kawamoto S, Saga T, Sato N, Hiraga A, Ishimori T, Konishi J, Togashi K, Brechbiel MW. Positive effects of polyethylene glycol conjugation to generation-4 polyamidoamine dendrimers as macromolecular MR contrast agents. Magn Reson Med 46:781–788, 2001.